



## Ni II 36 -Containing 54-Tungsto-6-Silicate: Synthesis, Structure, Magnetic and Electrochemical Studies

Joydeb Goura, Bassem S. Bassil, Xiang Ma, Ananthu Rajan, Eufemio Moreno-pineda, Jürgen Schnack, Masooma Ibrahim, Annie K. Powell, Mario Ruben, Jingjing Wang, et al.

### ► To cite this version:

Joydeb Goura, Bassem S. Bassil, Xiang Ma, Ananthu Rajan, Eufemio Moreno-pineda, et al.. Ni II 36 -Containing 54-Tungsto-6-Silicate: Synthesis, Structure, Magnetic and Electrochemical Studies. *Chemistry - A European Journal*, 2021, 27 (61), pp.15081-15085. 10.1002/chem.202102973 . hal-03594805

HAL Id: hal-03594805

<https://hal.science/hal-03594805>

Submitted on 2 Mar 2022

**HAL** is a multi-disciplinary open access archive for the deposit and dissemination of scientific research documents, whether they are published or not. The documents may come from teaching and research institutions in France or abroad, or from public or private research centers.

L'archive ouverte pluridisciplinaire **HAL**, est destinée au dépôt et à la diffusion de documents scientifiques de niveau recherche, publiés ou non, émanant des établissements d'enseignement et de recherche français ou étrangers, des laboratoires publics ou privés.

# Ni<sup>II</sup><sub>36</sub>-Containing 54-Tungsto-6-Silicate: Synthesis, Structure, Magnetic and Electrochemical Studies

Joydeb Goura,<sup>[a]</sup> Bassem S. Bassil,<sup>[a, b]</sup> Xiang Ma,<sup>[a]</sup> Ananthu Rajan,<sup>[a]</sup> Eufemio Moreno-Pineda,<sup>[c, d]</sup> Jürgen Schnack,<sup>[e]</sup> Masooma Ibrahim,<sup>[d]</sup> Annie K. Powell,<sup>[d, f]</sup> Mario Ruben,<sup>[d, g, h]</sup> Jingjing Wang,<sup>[i]</sup> Laurent Ruhlmann,<sup>[i]</sup> and Ulrich Kortz<sup>\*[a]</sup>

**Abstract:** The 36-Ni<sup>II</sup>-containing 54-tungsto-6-silicate, [Ni<sub>36</sub>(OH)<sub>18</sub>(H<sub>2</sub>O)<sub>36</sub>(SiW<sub>9</sub>O<sub>34</sub>)<sub>6</sub>]<sup>6-</sup> (**Ni<sub>36</sub>**) was synthesized by a simple one-pot reaction of the Ni<sub>2</sub>-pivalate complex [Ni<sub>2</sub>(μ-OH<sub>2</sub>)(O<sub>2</sub>CCMe<sub>3</sub>)<sub>4</sub>(HO<sub>2</sub>CCMe<sub>3</sub>)<sub>4</sub>] with the trilacunary [SiW<sub>9</sub>O<sub>34</sub>]<sup>10-</sup> polyanion precursor in water and structurally characterized by a multitude of physicochemical techniques including single-crystal XRD, FTIR, TGA, elemental analysis, magnetic and electrochemical studies. Polyanion **Ni<sub>36</sub>** comprises six equivalent {Ni<sub>6</sub>} units which are linked by Ni—O—W bridges forming a macrocyclic assembly. Magnetic studies demonstrate that the {Ni<sub>6</sub>} building blocks in **Ni<sub>36</sub>** remain magnetically intact while forming a hexagonal ring with antiferromagnetic exchange interactions between adjacent {Ni<sub>6</sub>} units. Electrochemical studies indicate that the first reduction is reversible and associated with the W<sup>VIV</sup> couple, whereas the second reduction is irreversible attributed to the Ni<sup>II/0</sup> couple.

Polyoxometalates (POMs) are discrete, anionic metal-oxo clusters with a large variety of structures, compositions and physicochemical properties. While plenary POMs such as [XW<sub>12</sub>O<sub>40</sub>]<sup>n-</sup> (X = P, Si, Ge) are not reactive, lacunar derivatives such as the monolacunary [XW<sub>11</sub>O<sub>39</sub>]<sup>n-</sup> or trilacunary [XW<sub>9</sub>O<sub>34</sub>]<sup>n-</sup> (prepared by controlled base hydrolysis of the plenary precursor) are highly reactive towards oxophilic electrophiles such as *d* and *f* block metal ions.<sup>[1]</sup> For decades the synthesis of high-nucularity transition metal ion-containing POMs has received much attention, mainly aiming at novel structures with associated interesting magnetic, electrochemical, catalytic and biomedical properties.<sup>[2]</sup> From a magnetism point of view, high-nucularity magnetic POMs may possess large uniaxial anisotropy (*D*) and high-spin ground states (*S*), possibly resulting in single-molecule magnetic behaviour and relevance for high-density magnetic data storage and nanotechnology.<sup>[3]</sup> Some selected examples of high-nucularity, magnetic *d*-metal ion-containing POMs<sup>[4]</sup> are [Mn<sub>40</sub>P<sub>32</sub>W<sub>224</sub>O<sub>888</sub>]<sup>144-</sup>,<sup>[4c]</sup> [Mn<sub>19</sub>(OH)<sub>12</sub>(SiW<sub>10</sub>O<sub>37</sub>)<sub>6</sub>]<sup>34-</sup>,<sup>[4e]</sup> [Fe<sub>48</sub>(OH)<sub>76</sub>(H<sub>2</sub>O)<sub>16</sub>(H<sub>2</sub>P<sub>2</sub>W<sub>12</sub>O<sub>48</sub>)<sub>8</sub>]<sup>28-</sup>,<sup>[4a]</sup> [Fe<sub>28</sub>P<sub>8</sub>W<sub>48</sub>O<sub>248</sub>H<sub>56</sub>]<sup>28-</sup>,<sup>[4g]</sup>

[a] Dr. J. Goura, Dr. B. S. Bassil, X. Ma, A. Rajan, Prof. U. Kortz

Department of Life Sciences and Chemistry  
Jacobs University  
Campus Ring 1, 28759 Bremen (Germany)  
E-mail: u.kortz@jacobs-university.de  
Homepage: <http://ukortz.user.jacobs-university.de/>

[b] Dr. B. S. Bassil

Department of Chemistry  
Faculty of Arts and Sciences  
University of Balamand, Tripoli (Lebanon)

[c] Dr. E. Moreno-Pineda

Departamento de Química-Física  
Escuela de Química  
Facultad de Ciencias Naturales, Exactas y Tecnología  
Universidad de Panamá (Panamá)

[d] Dr. E. Moreno-Pineda, Dr. M. Ibrahim, Prof. A. K. Powell, Prof. M. Ruben

Institute of Nanotechnology  
Karlsruhe Institute of Technology (KIT)  
76344 Eggenstein-Leopoldshafen (Germany)

[e] Prof. J. Schnack

Faculty of Physics  
Bielefeld University  
P.O. Box 100131, 33501 Bielefeld (Germany)

[f] Prof. A. K. Powell

Institute of Inorganic Chemistry  
Karlsruhe Institute of Technology (KIT)  
Engesserstrasse 15, 76131 Karlsruhe (Germany)

[g] Prof. M. Ruben

Institute for Quantum Materials and Technologies (IQMT)  
Karlsruhe Institute of Technology (KIT)  
Hermann-von-Helmholtz-Platz 1, 76344, Eggenstein-Leopoldshafen (Germany)

[h] Prof. M. Ruben

Centre Européen de Sciences Quantiques (CESQ)  
Institut de Science et d'Ingénierie Supramoléculaire (ISIS)  
8, Allée Gaspard Monge, 67000 Strasbourg (France)

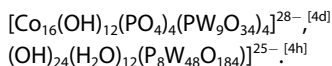
[i] J. Wang, Prof. L. Ruhlmann

Laboratoire d'Electrochimie et de Chimie Physique du Corps Solide  
Université de Strasbourg, Institut de Chimie  
UMR CNRS 7177, 4 rue Blaise Pascal  
CS 90032, 67081 Strasbourg cedex (France)

Supporting information for this article is available on the WWW under <https://doi.org/10.1002/chem.202102973>

This manuscript is part of a Special Issue "Cooperative effects in heterometallic complexes".

© 2021 The Authors. Chemistry - A European Journal published by Wiley-VCH GmbH. This is an open access article under the terms of the Creative Commons Attribution Non-Commercial NoDerivs License, which permits use and distribution in any medium, provided the original work is properly cited, the use is non-commercial and no modifications or adaptations are made.



With respect to the synthesis of Ni<sup>II</sup>-containing POMs, several species with different nickel-nuclearities ranging from 2 to 40 have been reported.<sup>[5,6]</sup> Most of these species have a sandwich-type structure, with a recent member being the heptanuclear tungstosilicate  $[\text{Ni}_7(\text{OH})_6(\text{H}_2\text{O})_4(\text{SiW}_8\text{O}_{31})_2]^{12-}$ , which showed ferromagnetic coupling between the hydroxo-bridged Ni<sup>II</sup> centres.<sup>[5a]</sup> In 2013 the 14-nickel-containing  $[\text{Ni}_{14}(\text{OH})_6(\text{H}_2\text{O})_{10}(\text{HPO}_4)_4(\text{P}_2\text{W}_{15}\text{O}_{56})_4]^{34-}$  was reported,<sup>[5d]</sup> and in 2015 the 25-nickel-containing  $[\text{Ni}_{25}(\text{OH})_{18}(\text{H}_2\text{O})_2(\text{CO}_3)_2(\text{PO}_4)_6(\text{SiW}_9\text{O}_{34})_6]^{50-}$ .<sup>[5b]</sup> Most of the known examples involve bridging secondary ligands such as HPO<sub>4</sub><sup>2-</sup>, PO<sub>4</sub><sup>3-</sup>, BO<sub>3</sub><sup>3-</sup> or CO<sub>3</sub><sup>2-</sup>.<sup>[5]</sup> Some POMs contain {Ni<sub>6</sub>XW<sub>9</sub>} (X=P, Si, Ge) units, which are connected to adjacent units via Ni—O=W bonds, resulting in different topologies.<sup>[6a-e]</sup> The hydroxo-bridged {Ni<sub>6</sub>} subunit represents a key fragment of the brucite-type sheet structure, which has also been observed in  $[\text{Mn}_{19}(\text{OH})_{12}(\text{SiW}_{10}\text{O}_{37})_6]^{34-}$  ( $\{\text{Mn}_{19}\}$ ).<sup>[4e]</sup> Interestingly, Long et al. used a Zr<sub>6</sub>O<sub>4</sub>(OH)<sub>4</sub>(bpydc)<sub>6</sub> “lacunary” MOF to capture  $\{\text{M}_{19}\}$  brucite-type sheet structures, very similar to the  $\{\text{Mn}_{19}\}$  sheets, but with halide bridges rather than OH. This resembles the situation in MX<sub>2</sub> solid-state structures in general for X=Cl, Br, I, and OH. In general, the occupancy is around 13–17, out of the maximum calculated 19. This suggests that using lacunary POMs as capping groups is a more robust strategy than trying to fill “holes” in MOF structures, as there are no defects in the former.<sup>[6b]</sup>

Here we report on the synthesis of a 36 Ni<sup>II</sup>-containing POM comprising exclusively trilacunary 9-tungstosilicate ions and hydroxo ligands. Reaction of the dinuclear coordination complex  $[\text{Ni}_2(\mu-\text{OH}_2)(\text{O}_2\text{CCMe}_3)_4(\text{HO}_2\text{CCMe}_3)_4]$  (Ni<sub>2</sub>-Piv) (Piv=HO<sub>2</sub>CCMe<sub>3</sub>)<sup>[7]</sup> with the trilacunary 9-tungstosilicate [SiW<sub>9</sub>O<sub>34</sub>]<sup>10-</sup> in water under hydrothermal conditions resulted in the formation of  $[\text{Ni}_{36}(\text{OH})_{18}(\text{H}_2\text{O})_{36}(\text{SiW}_9\text{O}_{34})_6]^{56-}$  (Ni<sub>36</sub>), which was isolated as a hydrated sodium salt, Na<sub>6</sub>[Ni<sub>36</sub>(OH)<sub>18</sub>(H<sub>2</sub>O)<sub>36</sub>(SiW<sub>9</sub>O<sub>34</sub>)<sub>6</sub>]·10·H<sub>2</sub>O (Na-Ni<sub>36</sub>). The title compound was characterized by a multitude of physicochemical techniques including single-crystal XRD, IR, TGA, elemental analysis, magnetic and electrochemical studies. Single-crystal XRD revealed that Na-Ni<sub>36</sub> crystallized in the triclinic system with space group P1. The crystallographic parameters are shown in the Supporting Information (Table S1). The polyanion Ni<sub>36</sub> consists of six {Ni<sub>6</sub>SiW<sub>9</sub>} subunits, each comprising a trilacunary {B- $\alpha$ -SiW<sub>9</sub>} Keggin unit with six incorporated Ni<sup>II</sup> ions coordinated octahedrally and bridged to each other by hydroxo ligands, and arranged in a coplanar fashion (Figure 1). The six {Ni<sub>6</sub>SiW<sub>9</sub>} subunits are connected to each other via Ni—O=W bonds, leading to a cyclic assembly with the {Ni<sub>6</sub>SiW<sub>9</sub>} subunits alternatingly pointing up and down, resulting in polyanion Ni<sub>36</sub> with S<sub>6</sub> point group symmetry. Interestingly, a side view of Ni<sub>36</sub> reveals six, planar {Ni<sub>6</sub>} assemblies arranged in a coplanar cyclic fashion and sandwiched by three {B- $\alpha$ -SiW<sub>9</sub>} units from above and below, respectively. Bond valence sum (BVS) calculations confirm that all the 36 nickel ions in Ni<sub>36</sub> have a +2 oxidation state (Table S2), and that the bridging oxygens are monoprotonated and hence hydroxo groups (Table S3).<sup>[8]</sup> A close inspec-

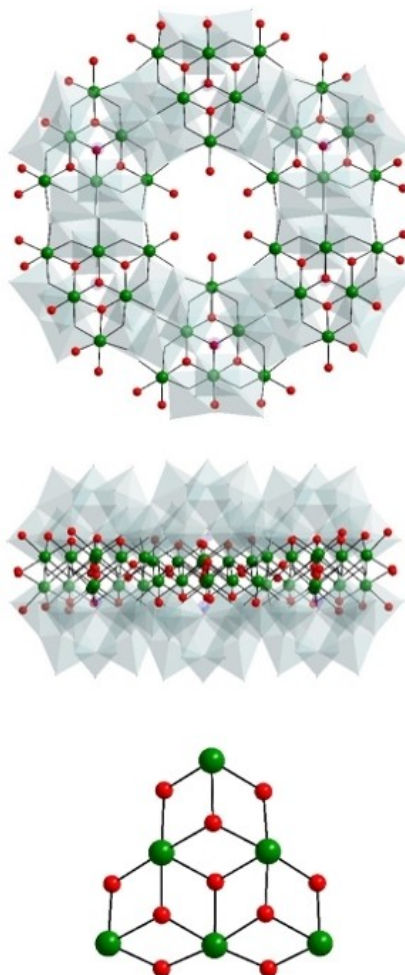


**Figure 1.** Structural representation of Ni<sub>36</sub> in top view (top), side view (middle), and one of the six hydroxo-bridged {Ni<sub>6</sub>} subunits (bottom). Color code: nickel (green), oxygen (red). The WO<sub>6</sub> octahedra and Si heteroatoms are shown as transparent octahedra and balls, respectively, to highlight the six {Ni<sub>6</sub>} subunits within Ni<sub>36</sub>.

tion of the {Ni<sub>6</sub>SiW<sub>9</sub>} subunits in Ni<sub>36</sub> indicates that each planar Ni<sub>6</sub>-hydroxo cluster comprises four interconnected Ni<sub>3</sub>O<sub>4</sub> cubane units. Such Ni<sub>3</sub>O<sub>4</sub> or Ni<sub>4</sub>O<sub>4</sub> motifs are known in POM chemistry as well as in coordination complexes.<sup>[9]</sup>

The magnetic properties of Na-Ni<sub>36</sub> have been measured in powdered sample employing a SQUID magnetometer, in the temperature range of 2 to 300 K and fields ranging from 0 to 7 T. The  $\chi T$  at room temperature is 53.1 cm<sup>3</sup> mol<sup>-1</sup> K, which is in the expected range for six uncoupled Ni<sub>6</sub> units.<sup>[10]</sup> Upon cooling, the  $\chi T$  profile increases, reaching a maximum  $\chi T$  value of 81.1 cm<sup>3</sup> at ca. 40 K, before decreasing to 13.2 cm<sup>3</sup> mol<sup>-1</sup> K at 2 K. The upsurge indicates the existence of ferromagnetic interactions, as observed within the composing Ni<sub>6</sub> units. The M(B) plot shows no saturation of the magnetization, with an almost linear profile with increasing field. Expectations were that the magnetism of Ni<sub>36</sub> is equal to that of its six uncoupled independent Ni<sub>6</sub> subunits. Both,  $\chi T$  versus  $T$  as well as  $M$  versus  $B$ , see Figure 2, suggest that there is a small exchange interaction through O—W—O bridges that couple adjacent Ni<sub>6</sub>

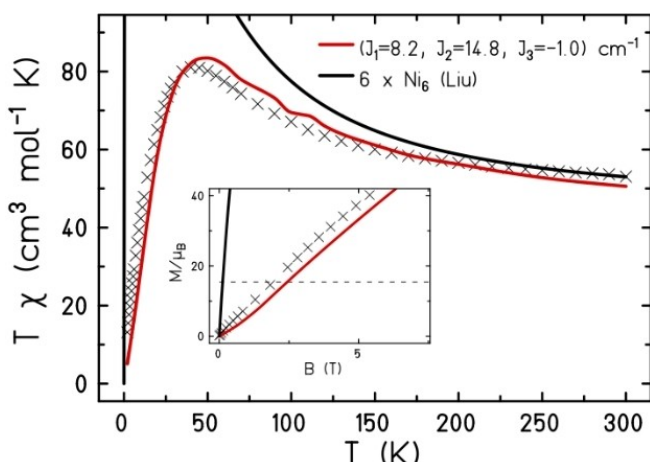


**Figure 2.** Magnetic susceptibility at  $B=0.1$  T and magnetization at  $T=2.0$  K (inset) – experimental data (symbols), ALPS QMC simulation (red curves), simulations of 6 independent  $\text{Ni}_6$  subunits (black curves).

triangles. We model this interaction by a single exchange integral  $J_3$  (blue in Figure 3), while leaving  $J_1$  and  $J_2$  as previously derived from the magnetism of the  $\text{Ni}_6$  subunits.<sup>[11]</sup>

The magnetism of discrete molecular objects as large as  $\text{Ni}_{36}$  cannot be modelled by exact diagonalization due to a prohibitive size of the related Hilbert space.<sup>[12]</sup> However, the magnetic interactions of  $\text{Ni}_{36}$  are non-frustrating since  $J_1$  and  $J_2$  are ferromagnetic and only  $J_3$  is antiferromagnetic; therefore, quantum Monte Carlo (QMC) calculations can be used. We simulated the magnetic observables using the program *dirloop\_sse* of the ALPS package.<sup>[13]</sup> As a result, we found that a weak antiferromagnetic exchange  $J_3=-1 \text{ cm}^{-1}$  connects neighboring subunits. The agreement with the experimental data is very good. Small deviations may result from not considered Ni anisotropies, possible modifications of  $J_1$  or  $J_2$ , or an exchange pattern that differs from Figure 3. The tiny wiggles of the red curves are due to the fact that the QMC calculations are not yet fully converged, even after several days of simulation.

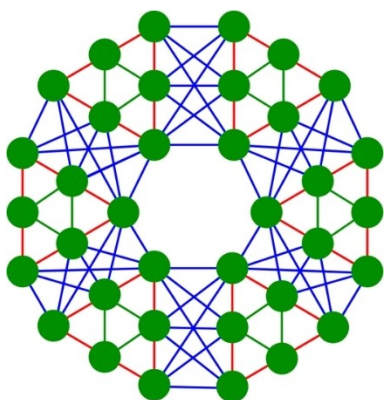


**Figure 3.** Schematic representation of exchange interactions in  $\text{Ni}_{36}$ :  $J_1$  (red) and  $J_2$  (green) as in Liu,<sup>[10]</sup>  $J_3$  (blue) denotes the exchange between adjacent  $\{\text{Ni}_6\}$  triangles. A “ $-2J$ ”-Hamiltonian was employed in the calculations.

The electrochemistry of  $\text{Na-Ni}_{36}$  was carried out in aqueous solutions in a pH 7.8 acetate medium, which is close to the pH used for the synthesis. For this purpose, the stability of polyanion  $\text{Ni}_{36}$  was assessed by cyclic voltammetry (CV). Only the tungsten centers are expected to give rise to an electrochemical response, with the  $\text{Ni}^{II}$  ions being silent at our experimental conditions.<sup>[14]</sup> The solid  $\text{Na-Ni}_{36}$  was first immobilized on the surface of the basal plane of the pyrolytic graphite disk (PGB) and the electrochemical responses studied in pH 7.8 acetate medium. Figure 4A and B features the CVs of  $\text{Ni}_{36}$  obtained at  $20 \text{ mV s}^{-1}$ , at two different reverse potentials in a pH 7.8 acetate medium. The CV of  $\text{Ni}_{36}$  exhibits a quasi-reversible reduction wave at  $-0.980 \text{ V}$  versus SCE (step I), followed by the second irreversible wave at  $-1.232 \text{ V}$  versus SCE (step II), which is very close to the solvent discharge. As shown in Figure 4B (dark-blue and dark-red curves), nearly the same cyclic voltammograms were measured after the first and the second scan without polishing the electrode showing the chemically reversible W-reduction at  $-0.980 \text{ V}$  versus SCE for the first step. In contrast, the second reduction (step II) corresponds to an irreversible multielectron transfer (Figure S3, blue curve). It must be noted that at the reverse sweep, one additional anodic peak at  $-0.502 \text{ V}$  versus SCE appeared (peak \*). It corresponds to the anodic dissolution peak of  $\text{Ni}^0$  and indicates that during the second irreversible reduction at

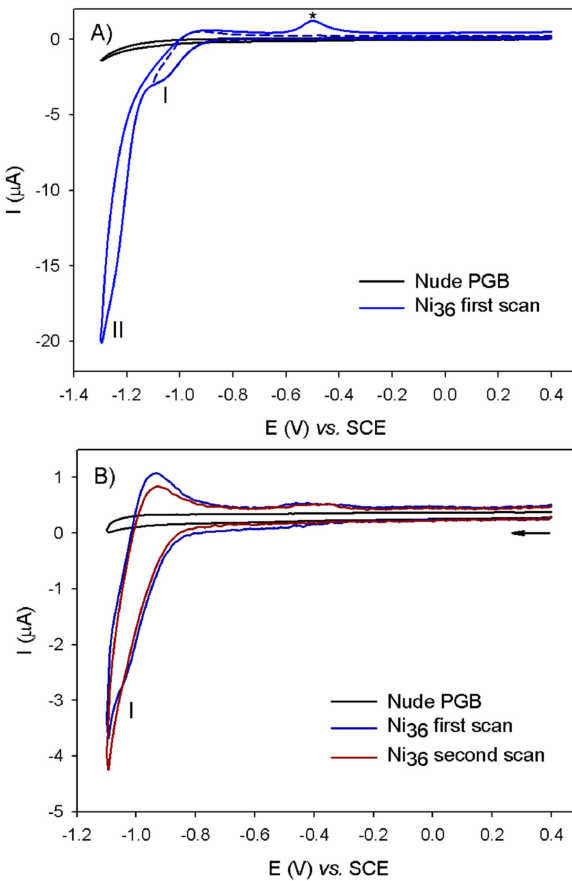


**Figure 4.** Cyclic voltammograms of  $\text{Na-Ni}_{36}$  immobilized at a PGB electrode ( $d=2 \text{ mm}$ ) in a  $1 \text{ M}$  pH 7.8 LiOAc-HAcO solution. Scan rate:  $20 \text{ mV s}^{-1}$ .

–1.232 versus SCE, reduction of Ni<sup>II</sup> to Ni<sup>0</sup> occurred, leading to decomposition of Ni<sub>36</sub>, but only during the second reduction.

Comparable measurements on a 0.50 mM solution of Ni<sub>36</sub> were obtained using a glassy carbon electrode (GC) in acetate medium at pH 7.8, as shown in Figure S4 (see Supporting Information). After polishing the GC electrode, similar CV curves were always obtained, even after 1 day. Moreover, no change of the UV-visible spectrum was observed (Figure S6). These results indicate that Ni<sub>36</sub> is stable in acetate medium at pH 7.8.

In summary, we have synthesized and structurally characterized the 36 Ni<sup>II</sup>-containing discrete, cyclic polyanion Ni<sub>36</sub>, which not only contains a record number of Ni<sup>II</sup> ions, but the magnetic core is constructed without the need for any secondary bridging capping groups such as phosphate, borate or carbonate. The title polyanion Ni<sub>36</sub> is prepared by reaction of the dinuclear coordination complex Ni<sub>2</sub>-Piv with the trilacunary {SiW<sub>9</sub>} Keggin polyanion precursor in water, and heating in a stainless-steel autoclave under autogenous pressure at 140 °C for three days. The structure of Ni<sub>36</sub> can be rationalized as a cyclic assembly of six identical {Ni<sub>6</sub>SiW<sub>9</sub>} units, which are oriented in alternating up/down orientations, resulting in a structure with S<sub>6</sub> symmetry. The magnetic properties of Ni<sub>36</sub> result from the combined action of ferromagnetic exchange interactions within the {Ni<sub>6</sub>} units, as well as antiferromagnetic exchange interactions between neighboring {Ni<sub>6</sub>} units. For low temperatures and fields this qualitatively corresponds to a hexagonal ring of weakly antiferromagnetically interacting {Ni<sub>6</sub>} units, each {Ni<sub>6</sub>} unit possessing an effective spin S=6. The electrochemical properties indicate a good stability of Ni<sub>36</sub> toward the first reduction step, which is almost reversible, whereas the polyanion decomposes at the second reduction step, due to the reduction of Ni<sup>II</sup> to Ni<sup>0</sup>.

## Experimental Section

**Synthesis of Na<sub>6</sub>[Ni<sub>36</sub>(H<sub>2</sub>O)<sub>36</sub>(OH)<sub>18</sub>(SiW<sub>9</sub>O<sub>34</sub>)<sub>6</sub>] · 105H<sub>2</sub>O (Na-Ni<sub>36</sub>):** The coordination complex [Ni<sub>2</sub>(μ-OH)<sub>2</sub>(O<sub>2</sub>CCMe<sub>3</sub>)<sub>4</sub>(HO<sub>2</sub>CCMe<sub>3</sub>)<sub>4</sub>] (Ni<sub>2</sub>-Piv) (Piv=HO<sub>2</sub>CCMe<sub>3</sub>)<sup>[7]</sup> (0.255 g, 0.272 mmol) was dissolved in H<sub>2</sub>O (40 mL) and then Na<sub>10</sub>[A-α-SiW<sub>9</sub>O<sub>34</sub>]·24H<sub>2</sub>O (0.200 g, 0.068 mmol)<sup>[15]</sup> was added with constant stirring for 10 min at room temperature. The resultant reaction mixture was transferred into a Teflon-lined stainless-steel autoclave and was heated under autogenous pressure at 140 °C for three days. After overnight cooling a precipitate had formed at the bottom of the Teflon container, which was removed by centrifugation and/or filtration. The solution was kept in an open vial at room temperature to allow for slow evaporation. After about one month a green, crystalline product started to appear. Evaporation was allowed to continue until most of the solvent had disappeared. Then the solid product was collected by filtration and air dried. Yield 15 mg (7%, based on W). IR (2% KBr pellet):  $\tilde{\nu}$ =3412(br), 1619(s), 1379(sh), 947(s), 878(s), 833(sh), 790(s), 687(s), 541(w), 513(w), 478(sh). Elemental analysis (%) for Na<sub>6</sub>[Ni<sub>36</sub>(H<sub>2</sub>O)<sub>36</sub>(OH)<sub>18</sub>(SiW<sub>9</sub>O<sub>34</sub>)<sub>6</sub>] · 105H<sub>2</sub>O (Na-Ni<sub>36</sub>), calcd: W 53.79, Ni 11.45, Na 0.75, Si 0.91; found W 51.35, Ni 12.02, Na 0.78, Si 0.77. Elemental analysis was performed at CREALINS (Villeurbanne, France), except for Na, which was determined by atomic absorption at Jacobs University.

Deposition Number 2001196 (Na-Ni<sub>36</sub>) contains the supplementary crystallographic data for this paper. These data are provided free of

charge by the joint Cambridge Crystallographic Data Centre and Fachinformationszentrum Karlsruhe Access Structures service www.ccdc.cam.ac.uk/structures.

## Acknowledgements

U.K. thanks the German Science Foundation (DFG, KO 2288/20-1), the CMST COST Action CM1203 (PoCheMoN), and Jacobs University for research support. L.R. thanks CNRS, the Université de Strasbourg (France) for the project “Idex Attractivité” as well as the Labex CSC (Chemistry of Complex Systems), which has also supported one part of this research. EMP thanks the Panamanian National System of Investigators (SNI, SENACYT) for support. Figure 1 was generated using *Diamond*, Version 3.2 (copyright Crystal Impact GbR). Open Access funding enabled and organized by Projekt DEAL.

## Conflict of Interest

The authors declare no conflict of interest.

**Keywords:** Electrochemistry · magnetic properties · nickel · polyoxometalates · structure elucidation

- [1] a) M. T. Pope, U. Kortz, Polyoxometalates, *Encyclopedia of Inorganic and Bioinorganic Chemistry* 2012, John Wiley & Sons, Ltd.:Hoboken, NJ, <https://doi.org/10.1002/9781119951438.eibc0185.pub2>; b) M. T. Pope, A. Müller, *Angew. Chem. Int. Ed. Engl.* 1991, 30, 34–48; c) M. T. Pope, *Heteropoly and Isopoly Oxometalates*, Springer, Berlin, 1983.
- [2] a) A. V. Anyushin, A. Kondinski, T. N. Parac-Vogt, *Chem. Soc. Rev.* 2020, 49, 382–432; b) L. Chen, W. L. Chen, X. L. Wang, Y. G. Li, Z. M. Su, E. B. Wang, *Chem. Soc. Rev.* 2019, 48, 260–284; c) K. P. Sullivan, Q. Yin, D. L. Collins-Wildman, M. Tao, Y. V. Geletii, D. G. Musaev, T. Lian, C. L. Hill, *Front. Chem.* 2018, 6, 1–10; d) C. Boskovic, *Acc. Chem. Res.* 2017, 50, 2205–2214; e) O. Oms, A. Dolbecq, P. Mialane, *Chem. Soc. Rev.* 2012, 41, 7497–7536; f) C. L. Hill, *Chem. Rev.* 1998, 98; g) S. G. Sarafianos, U. Kortz, M. T. Pope, M. J. Modak, *Biochem. J.* 1996, 319, 619–626.
- [3] a) E. Coronado, *Nat. Rev. Mater.* 2020, 5, 87–104; b) M. Ibrahim, V. Mereacre, N. Leblanc, W. Wernsdorfer, C. E. Anson, A. K. Powell, *Angew. Chem.* 2015, 127, 15795–15799; *Angew. Chem. Int. Ed.* 2015, 54, 15574–15578; c) Z.-M. Zhang, S. Yao, Y.-G. Li, H.-H. Wu, Y.-H. Wang, M. Rouzières, R. Clérac, Z.-M. Su, E.-B. Wang, *Chem. Commun.* 2013, 49, 2515–2517; d) X. Fang, P. Kögerler, M. Speldrich, H. Schilder, M. Luban, *Chem. Commun.* 2012, 48, 1218–1220; e) J. M. Clemente-Juan, E. Coronado, A. Gaia-Ariño, *Chem. Soc. Rev.* 2012, 41, 7464–7478; f) J.-D. Compain, P. Mialane, A. Dolbecq, I. M. Mbomekallé, J. Marot, F. Sécheresse, E. Rivière, G. Rogez, W. Wernsdorfer, *Angew. Chem.* 2009, 121, 3123–3127; *Angew. Chem. Int. Ed.* 2009, 48, 3077–3081; g) U. Kortz, A. Müller, J. van Slageren, J. Schnack, N. S. Dalal, M. Dressel, *Coord. Chem. Rev.* 2009, 293, 2315–2327; h) E. Coronado, P. Day, *Chem. Rev.* 2004, 104, 5419–5448.
- [4] a) J. Goura, J. K. Bindra, I. A. Rutkowska, P. J. Kulesza, N. S. Dalal, U. Kortz, *Chem. Eur. J.* 2020, 26, 15821–15824; b) C. Zhang, M. Zhang, H. Shi, Q. Zeng, D. Zhang, Y. Zhao, Y. Wang, P. Ma, J. Wang, J. Niu, *Chem. Commun.* 2018, 54, 5458–5461; c) X. Fang, P. Kögerler, Y. Furukawa, M. Speldrich, M. Luban, *Angew. Chem.* 2011, 123, 5318–5322; *Angew. Chem. Int. Ed.* 2011, 50, 5212–5216; d) M. Ibrahim, Y. Lan, B. S. Bassil, Y. Xiang, A. Suchopar, A. K. Powell, U. Kortz, *Angew. Chem.* 2011, 123, 4805–4808; *Angew. Chem. Int. Ed.* 2011, 50, 4708–4711; e) B. S. Bassil, M. Ibrahim, R. Al-Oweini, M. Asano, Z. Wang, J. van Tol, N. S. Dalal, K.-Y. Choi, R. Ngo Biboum, B. Keita, L. Nadjo, U. Kortz, *Angew. Chem.* 2011, 123, 6083–6087; *Angew. Chem. Int. Ed.* 2011, 50, 5961–5964; f) C. Ritchie, A. Ferguson, H. Nojiri, H. N. Miras, Y.-F. Song, D.-L. Long, E. Burkholder, M. Murrie, P. Kögerler, E. K. Brechin, L. Cronin, *Angew. Chem.* 2008, 120,

- 5691–5694; *Angew. Chem. Int. Ed.* **2008**, *47*, 5609–5612; g) B. Godin, Y.-G. Chen, J. Vaissermann, L. Ruhlmann, M. Verdaguer, P. Gouzerh, *Angew. Chem.* **2005**, *117*, 3132–3135; *Angew. Chem. Int. Ed.* **2005**, *44*, 3072–3075; h) S. S. Mal, U. Kortz, *Angew. Chem.* **2005**, *117*, 3843–3846; *Angew. Chem. Int. Ed.* **2005**, *44*, 3777–3780.
- [5] a) B. S. Bassil, Y. Xiang, A. Haider, J. Hurtado, G. Novitchi, A. K. Powell, A. M. Bossoh, I. M. Mbomekallé, P. de Oliveira, U. Kortz, *Chem. Commun.* **2016**, *52*, 2601–2604; b) X.-B. Han, Y.-G. Li, Z.-M. Zhang, H.-Q. Tan, Y. Lu, E.-B. Wang, *J. Am. Chem. Soc.* **2015**, *137*, 5486–5493; c) S. Li, S. Liu, Q. Tang, Y. Liu, D. He, S. Wang, Z. Shi, *Dalton Trans.* **2013**, *42*, 13319–13322; d) M. Ibrahim, Y. Xiang, B. S. Bassil, Y. Lan, A. K. Powell, P. de Oliveira, B. Keita, U. Kortz, *Inorg. Chem.* **2013**, *52*, 8399–8408; e) N. H. Nsouli, M. Prinz, N. Damnik, M. Neumann, E. Talik, U. Kortz, *Eur. J. Inorg. Chem.* **2009**, *36*, 5096–5101; f) C. Pichon, P. Mialane, A. Dolbecq, J. Marrot, E. Rivière, B. S. Bassil, U. Kortz, B. Keita, L. Nadjo, F. Sécheresse, *Inorg. Chem.* **2008**, *47*, 11120–11128; g) Z. Zhang, Y. Li, E. Wang, X. Wang, C. Qin, *Inorg. Chem.* **2006**, *45*, 4313–4315; h) U. Kortz, I. M. Mbomekalle, B. Keita, L. Nadjo, P. Berthet, *Inorg. Chem.* **2002**, *41*, 6412–6416; i) U. Kortz, A. Tézé, G. Hervé, *Inorg. Chem.* **1999**, *38*, 2038–2042; j) J. M. Clemente-Juan, E. Coronado, J. R. Galán-Mascarós, C. J. Gómez-García, *Inorg. Chem.* **1999**, *38*, 55–63.
- [6] a) Y. Chen, Z. W. Guo, Y. P. Chen, Z. Y. Zhuang, G. Q. Wang, X. X. Li, S. T. Zheng, G. Y. Yang, *Inorg. Chem. Front.* **2021**, *8*, 1303 and references therein; b) M. I. Gonzalez, A. B. Turkiewicz, L. E. Darago, J. Oktawiec, K. Bustillo, F. Grandjean, G. J. Long, J. R. Long, *Nature* **2020**, *577*, 64–68; c) Y. X. Yin, W. C. Chen, W. Yao, C. Qin, Z. M. Su, *CrystEngComm* **2018**, *20*, 7507; d) L. Huang, J. Zhang, L. Cheng, G. Y. Yang, *Chem. Commun.* **2012**, *48*, 9658–9660; e) S. T. Zheng, J. Zhang, G. Y. Yang, *Angew. Chem.* **2008**, *120*, 3973–3977; *Angew. Chem. Int. Ed.* **2008**, *47*, 3909–3913; f) S. T. Zheng, D. Q. Yuan, H. P. Jia, J. Zhang, G. Y. Yang, *Chem. Commun.* **2007**, 1858–1860.
- [7] G. Chaboussant, R. Basler, H.-U. Güdel, S. Ochsenbein, A. Parkin, S. Parsons, G. Rajaraman, A. Sieber, A. A. Smith, G. A. Timco, R. E. P. Winpenny, *Dalton Trans.* **2004**, 2758–2766.
- [8] I. D. Brown, D. Altermatt, *Acta Crystallogr. Sect. B* **1985**, *41*, 244–247.
- [9] a) A. Das, F. J. Klinke, S. Demeshko, S. Meyer, S. Dechert, F. Meyer, *Inorg. Chem.* **2012**, *51*, 8141–8149; b) S. Petit, P. Neugebauer, G. Pilet, *Inorg. Chem.* **2012**, *51*, 6645–6654.
- [10] Y.-C. Liu, C.-H. Fu, S.-T. Zheng, J.-W. Zhao, G.-Y. Yang, *Dalton Trans.* **2013**, *42*, 16676–16679.
- [11] Our values of  $J_1$  and  $J_2$  are ten times larger than those given by Liu et al. (Ref. [9]). We speculate that it is a typo in their paper.
- [12] a) J. Schnack, *Contemp. Phys.* **2019**, *60*, 127–144; b) R. Schnalle, J. Schnack, *Int. Rev. Phys. Chem.* **2010**, *29*, 403–452.
- [13] a) B. Bauer, L. D. Carr, H. G. Evertz, A. Feiguin, J. Freire, S. Fuchs, L. Gamper, J. Gukelberger, E. Gull, S. Guertler, A. Hehn, R. Igarashi, S. V. Isakov, D. Koop, P. N. Ma, P. Mates, H. Matsuo, O. Parcollet, G. Pawłowski, J. D. Picon, L. Pollet, E. Santos, V. W. Scarola, U. Schollwöck, C. Silva, B. Surer, S. Todo, S. Trebst, M. Troyer, M. L. Wall, P. Werner, S. Wessel. The ALPS project release 2.0: open source software for strongly correlated systems. *J. Stat. Mech.* **2011**, P05001; b) A. F. Albuquerque, F. Alet, P. Corboz, P. Dayal, A. Feiguin, S. Fuchs, L. Gamper, E. Gull, S. Gürler, A. Honecker, R. Igarashi, M. Körner, A. Kozhevnikov, A. Läuchli, S. R. Manmana, M. Matsumoto, I. P. McCulloch, F. Michel, R. M. Noack, G. Pawłowski, L. Pollett, T. Pruschke, U. Schollwöck, S. Todo, S. Trebst, M. Troyer, P. Werner, S. Wessel. The ALPS project release 1.3: Open-source software for strongly correlated systems. *J. Magn. Magn. Mater.* **2007**, *310*, 1187–1193.
- [14] B. Keita, L. Nadjo, Electrochemistry of Polyoxometalates, *Encyclopedia of Electrochemistry*; A. J. Bard, M. Stratmann, Eds., Wiley-VCH: **2006**, Vol. 7, p 607.
- [15] a) *Inorganic Syntheses*; A. P. Ginsberg, Ed.; Wiley VCH: New York, **1990**; b) G. Hervé, A. Tézé, *Inorg. Chem.* **1977**, *16*, 2115–2117.

Manuscript received: August 15, 2021

Accepted manuscript online: August 20, 2021

Version of record online: September 22, 2021